# Pore scale numerical modeling of bacterial growth and decay in Cr VI reactive transport

Apoorva Pallepati

A Dissertation Submitted to

Indian Institute of Technology Hyderabad

In Partial Fulfillment of the Requirements for

The Degree of Master of Technology



भारतीय प्रौद्योगिकी संस्थान हैदराबाद

**Indian Institute of Technology Hyderabad**

Department of Civil Engineering

June 2019

# Declaration

I declare that this written submission represents my ideas in my own words, and where others' ideas or words have been included, I have adequately cited and referenced the original sources. I also declare that I have adhered to all principles of academic honesty and integrity and have not misrepresented or fabricated or falsified any idea/data/fact/source in my submission. I understand that any violation of the above will be a cause for disciplinary action by the Institute and can also evoke penal action from the sources that have thus not been properly cited, or from whom proper permission has not been taken when needed.
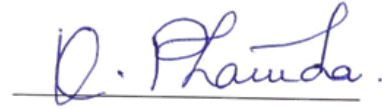
_(Signature)_

(Apoorva Pallepati)

(CE17AMTECH11006)

# Approval Sheet

This thesis entitled – Pore scale numerical modeling of bacterial growth and decay in Cr VI reactive transport – by – Apoorva Pallepati – is approved for the degree of Master of Technology from IIT Hyderabad.
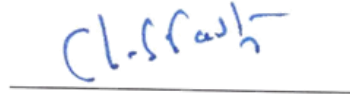
Dr.KBVN.Phanindra

Examiner

Shashidhar, Head and Associate Professor,

Department of Civil Engineering

Adviser

Prof.C.S.Shastri, Department of Mathematics

Chairman

iii

# Acknowledgments

Thank you very much.

Dedicated to


My family, my teachers and, my friends.

# Abstract

To understand the mechanism of bacteria growth in a reactive transport model inside a bio barrier for bioremediation, numerical modeling in the pore scale has to be done. An attempt has been made to understand and simulate the growth and decay of indigenous bacteria in a saturated porous medium at pore scale having a known concentration of Cr VI and to predict the enhanced microbial activity for the transformation of Cr VI to Cr III. Darcy scale models previously developed failed to address the hydrodynamics of the system, and contaminant degradation rates were over-predicted. In this study, the pore scale model combines processes such as fluid flow, solute transport with advection & diffusion equations of Cr VI reactive transport. Along with biotransformation of Cr VI and substrate consumption, the model majorly incorporates bacterial growth and decay on a pore scale. The model is divided into three portions, one for each of the processes and operated on different time scales. The mathematical equations are solved using FEM with appropriate initial and boundary conditions. The model developed can predict the velocity and pressure profiles developed fairly well. It can also predict the movement and, consumption of the substrate and biotransformation of Cr (VI) by bacteria along with the changes in its concentration.

Key words: biotransformation, pore scale modelling, finite element method

# Nomenclature

FEM: Finite Element Method

FVM: Finite Volume Method

FDM: Finite Difference Method

LBM: Lattice Boltzmann Method

PN: Pore Network

Cr: Chromium

# Contents

# List of Figures

# List of Tables

# Chapter 1

# Introduction

## 1.1    General Introduction

Unconstrained discharge of industrial effluents has contaminated the surrounding environment, along with the groundwater resources in the vicinity. The contaminants present in the effluent infiltrate inside the aquifer and travel long distances along with the water. Hence the contamination is not restricted to just the surroundings, but to a significant area covered by the aquifer.

Heavy metals like Cr (VI), its compounds used in tanning and electroplating industries have contaminated aquifers worldwide and it is crucial to remediate them. Cr (VI) is a highly toxic, water-soluble and highly mobile while its reduced form Cr (III) is less toxic and less soluble. Hence transforming Cr (VI) to Cr (III) is a way of remediation. This can be done in situ by injecting inorganic chemicals like iron sulphide or Cr (VI) reducing bacteria where reduction is carried out in the cell membrane or by enzyme reductase. [1]

Biotransformation can be aerobic/ anaerobic/ anoxic or combination of these three, based on the microorganisms. It has been reported that several microorganisms, under various environmental conditions, can reduce Cr (VI) to Cr (III) very effectively and modelling it requires adequate understanding of the bacterial behavioural interaction (growth pattern and chemotaxic response) with Cr (VI) and the nutrients present in the sub surface. Various factors that affect the biotransformation are biomass density, initial Cr (VI) concentration, carbon sources, pH, temperature, dissolved oxygen, oxidation and reduction potential (ORP), other oxyanions, and metal cations. [2]

For developing an effective bio barrier, approximate prediction on the microbial interaction at pore scale level must be grasped. Previous Darcy scale models of Cr (VI) reactive

biomass growth has helped in understanding the evolution of the sub-surface environment assuming that it is a continuum described with bulk parameters and that all the phases coexist at a point in space. On the other hand, pore scale is the largest spatial scale at which differentiation of fluid and solid phase is possible. As the pore scale accounts for the pore-space architecture where the microbial reactions and multicomponent transport occur, the biogeochemical behaviour that was not grasped or predicted using other scales can be explained.
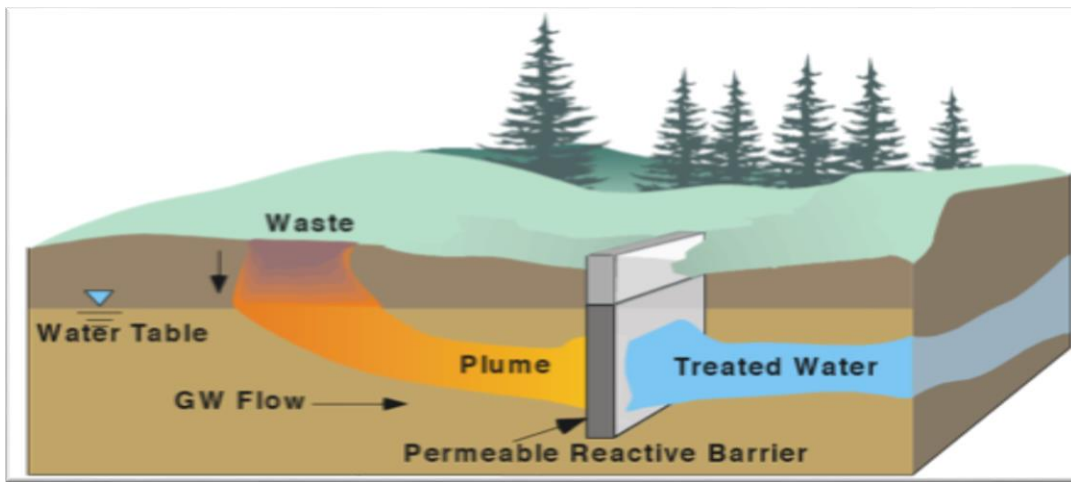


**Figure 1.1 Bio barrier**

In this study an attempt has been made to understand pore scale processes that take place in a bio barrier containing a bacterium consortium that reduce Cr (VI).

There are numerical methods like FEM, FDM, etc. that can be used to solve PDEs. In this model finite element method has been used to solve the equations

## 1.2    Purpose and scope of the project

- To understand the growth and decay of bacteria in Cr (VI) reactive transport in the micro scale and simulate it
- To use the model developed to explain the processes that occur in the pore scale experimental model
- To upscale a validated numerical pore scale model to the Darcy scale, simulate field conditions and help in designing an efficient and economical bio barrier.

## 1.3     Objectives

To develop 2D model of Cr (VI) reactive transport for a micro-scale model

- Model substrate flow using Navier-Stokes equation

- Model the change in concentrations of the substrate and Cr (VI) due to advection, diffusion and bio-transformation

- Using the velocity profile developed and Monod's equation to simulate bacteria spread and growth

## 1.4     Thesis outline

Chapter 1: Introduction

Chapter 1 gives a general introduction and background for the project along with the purpose of this project

Chapter 2: Literature Review

Chapter 2 gives an insight into the research and study done by research scholars on pore scale modeling of fluid flow, solute transport and biomass growth.

Chapter 3: Methodology

Chapter 3 describes Finite Element Method briefly

Chapter 4: Numerical Model

Chapter 4 describes the 2D pore scale model developed

Chapter 5: Results and discussions

# Chapter 2

# Literature Review

## 2.1 Biotransformation of Cr VI to Cr III

Cr VI conversion to Cr III can occur either inside the cell on in a solution by extra cellular enzymes. In situ remediation can be done by the introduction of nutrients (electron donors), microbes, or both. Several species of bacteria and algae are cultured in the laboratory so that the reduction is easier. [3]

## 2.2 Pore scale modeling of fluid

2D biomass growth model for a micro model was developed under three modules: fluid flow, solute transport and bacteria growth. A steady velocity stokes flow was established using LBM and FVM with upwind advective transport was used to numerically solve the advection-diffusion-reaction equation for the solutes used. Biomass transport was simulated using cellular automata and local growth rate of biomass in each computational cell was calculated using double Monod's equation. Local shear stress at each cell was calculated to compare with the maximum shear stress to determine direction of movement of biomass and de clogging of pores after decay of biomass. [4-5]

Steady state water flux in each pore throat was calculated using Hagen–Poiseuille equation and transport of solute was modeled using Monod type kinetics and mass conservation equations at different phases. The modeling was done using COMSOL. [6]

Combined finite element and finite volume method (FEFVM) can also be used. A model to simulate multiphase flow in a complex geologic media used node centered finite volumes with standard Galerkin solutions of the fluid equation, which allowed to efficient modeling of non-linear multiphase flow in a highly heterogeneous geologic media with complex structures. [7]

2D model multiphase model was developed to simulate fluid flow in a microfluidic model using STAR-CCM+ software that uses FVM on unstructured grids and the volume of fluid method to implicitly track the interface between two phases. Significant variations were observed when compared to experimental results during the imbibition stage. [8]

A multi component model using LBM was used to numerically solve fluid flow, solute transport and bacteria growth equations to develop a 2D model to simulate experimental results. Homogeneous reactions were described through local equilibrium mass action relations, while mineral reactions were treated kinetically through boundary conditions at the mineral surface. The model was further improved by incorporating distribution function boundary condition for the total solute concentration and compared to analytical solutions obtained from FLOTRAN and AQUASIM simulations. It was found that solute mass was strictly conserved in the new model. [9-13]


## 2.3 Pore scale modeling of biomass

A multispecies one-dimensional model was developed for a membrane based biofilm reactor that included dual substrate Monod kinetics for a steady state biofilm, to simulate the experimental model of the same. [9-10]

Extended FEM (XFEM) was used in a continuum model based on diffusion-reaction to simulate growth on agar substrate, which showed relationship between bacteria growth morphology and nutrient consumption. [14]

The primary weakness of using cellular automata to model microbial activity is that to obtain numerical solutions, rules governing the cell behavior must be specified and these rules are difficult to establish experimentally. [11]

FDM with central differences and both explicit and implicit schemes was used to numerically solve Monod kinetic equations along with equations for interfacial velocities to simulate biofilm growth in porous media. Homogenization was used to upscale the model. [15]

To check the influence of biomass growth on hydraulic properties of porous media, a two-dimensional network of interconnected pore elements was developed to simulate field conditions and it consisted of an aqueous phase, biofilm phase and a solid phase (pores). Aqueous flow was established using the classical form of Poiseuille equation, solute transport using 1D convection-diffusion-reaction equation and biomass growth using Monod type kinetics. [16]

It has been found that bacteria spreading are non-Fickian and it becomes intensely super diffusive with progressive bio clogging in the porous media indicating preferential flow

pathways and stagnation zones. Gamma distribution and Lagrangian velocity distributions were used and they provided parameters that quantify changes in the flow. Exponentially evolving hydrodynamic metrics agreed with a similar bacterial growth and was used to parameterize a continuous time random walk model with a stochastic velocity relaxation. [17]

A two-dimensional, reactive-transport pore-network model of the saturated porous environments was developed to investigate how the physical characteristics of a medium contribute to the transport mechanisms of nutrients and their consumption by the indigenous microorganisms. In addition, the effect from the spatial distribution of the microorganisms was also explored. Results show that the complex spatio-temporal distribution of nutrients is mainly driven by the interactions between the system's physical conditions, such as medium inherent heterogeneity, base flow residence time, the nutrient input concentrations, and the degradation capacity of the interior biomass. Simulation results also revealed that the spatial heterogeneity of the pore-sizes is a more potent regulator than the biomass dispersal in controlling the spatial distribution and transport of nutrients. [18]

# Chapter 3

# Methodology

Finite Element method was used in the model and the method is as follows

- Considering a simple advection-diffusion equation

$$\vec{u}.\nabla u - D\nabla^2 u = f \dots\dots\dots\dots\dots\dots\dots\dots\dots \qquad (1)$$

- Using Method of weighted Residuals,

$$\int_\Omega wR\, d\Omega = 0 \dots\dots\dots\dots\dots\dots\dots\dots\dots (2)$$

Where $R$ residual of the equation, $R = \vec{u}.\nabla u - D\nabla^2 u - f \;\dots..(3)$

and $w$ is the weight function

Thus the equation (1) is converted to its weak form

$$\int_\Omega \left( w\vec{u}.\nabla u - wD\nabla^2 u - wf \right) d\Omega = 0 \dots\dots\dots..(4)$$

- The diffusion term is integrated by parts to lower differentiation requirements of the unknown weighted residual.

$$\textbf{Hence} \quad \int_\Omega -wD\nabla^2 u\, d\Omega = \int_\Omega D\nabla w\nabla u\, d\Omega - \int_\Gamma wD(\vec{n}.\nabla u)\, d\Gamma \dots\dots\dots (5)$$

The last term of the above equation at the boundaries ($\Gamma$) of the domain ($\Omega$) and $\vec{n}$ is the unit outward normal of the boundary.

- Using Galerkin method, i.e. weight function is the same as shape (basis) function

$$w = S_i(x,y) \dots\dots\dots\dots\dots\dots\dots\dots\dots (6)$$

- Shape functions are nonzero only over the elements which are in contact with the node they are associated with, everywhere else they are zero. Hence they possess the Kronecker-delta property

$$S_j(x_i) = \delta_{ij} = \begin{cases} 1 \text{ if } i = j \\ 0 \text{ if } i \neq j \end{cases}$$

Which implies that the $j^{th}$ shape function has a value of 1 at the $j^{th}$ node of the mesh and is equal to zero at all other nodes.

- Approximate solution for $u$ is defined as a summation of product of unknown nodal values ($u_j$) and shape function $S_j$

$$u_{app}(x, y) = \sum_{j=1}^{NN} u_j S_j(x, y) \ldots \ldots \ldots \ldots \ldots \ldots \ldots \ldots (7)$$

  Where NN is the number of nodes (number of equations)

- Substituting equation (5), (6) and (7) in (4)

$$\sum_{j=1}^{NN} \left\{ \int_{\Omega} \left[ S_i \left( u_x \frac{\partial S_j}{\partial x} + u_y \frac{\partial S_j}{\partial y} \right) + D \left( \frac{\partial S_i}{\partial x} \frac{\partial S_j}{\partial x} + \frac{\partial S_i}{\partial x} \frac{\partial S_j}{\partial x} \right) \right] d\Omega \right\} u_j = \int_{\Omega} S_i f d\Omega + \int_{\Gamma} S_i (SV) d\Gamma$$

where $SV = D\vec{n}.\nabla u$ and $NN$: number of nodes

- FEM can be generalized as

$$[K]\{u\} = \{F\}$$

  Where $[K]$ is the stiffness matrix of order NN×NN, $\{u\}$ is the unknown column matrix and $\{F\}$ is force vector. Where each element of stiffness matrix, $K_{ij}$

$$K_{ij} = \int_{\Omega} \left[ S_i \left( u_x \frac{\partial S_j}{\partial x} + u_y \frac{\partial S_j}{\partial y} \right) + D \left( \frac{\partial S_i}{\partial x} \frac{\partial S_j}{\partial x} + \frac{\partial S_i}{\partial x} \frac{\partial S_j}{\partial x} \right) \right] d\Omega$$

- Two-dimensional 3 noded triangular and 4 noded quadrilateral elements have been used. The (**x,y**) coordinates are shifted to master element coordinates (**ξ,η**)
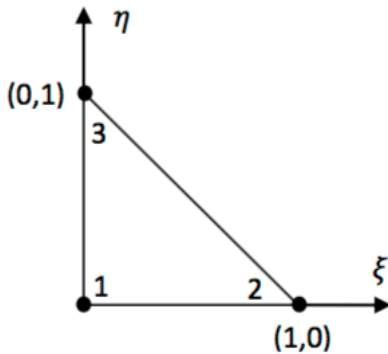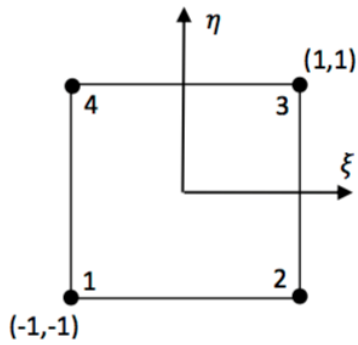
General form : $S = A + B\xi + C\eta$

$S_1 = 1 - \xi - \eta$

$S_2 = \xi$

$S_3 = \eta$

General form : $S = A + B\xi + C\eta + D\xi\eta$

$S_1 = \dfrac{1}{4}(1-\xi)(1-\eta)$ ,     $S_2 = \dfrac{1}{4}(1+\xi)(1-\eta)$

$S_3 = \dfrac{1}{4}(1+\xi)(1+\eta)$ ,     $S_4 = \dfrac{1}{4}(1-\xi)(1+\eta)$

- Gauss quadrature is a numerical integration technique that converts integral equations to a numerical form in which integrals are evaluated between -1 and 1, that can be coded.

General form of GQ: $\displaystyle\int_{-1}^{1} f(\xi)\,d\xi = \sum_{k=1}^{NGP} f(\xi_k)W_k$

NGP: Number of gauss points

$$x(\xi,\eta)= \sum_{j=1}^{NEN} x_j^e S_j(\xi,\eta) \quad , \quad y(\xi,\eta)= \sum_{j=1}^{NEN} y_j^e S_j(\xi,\eta)$$

Where NEN is the node number of element = 4 for quadrilateral element and 3 for triangular elements. And $x_j^e$ and $y_j^e$ are the nodal coordinates of the element.

As the shape function $S_j$ is used for both unknown approximation and coordinate transformation, it is known as iso-parametric formulation.

- The GQ points and weights for the elements are as follows

**Table 3.1 Gauss Quadrature and their weights for 4 noded quadrilateral and 3 noded triangular elements**

| NGP | $\xi_k$ | $\eta_k$ | $W_k$ |
|---|---|---|---|
| 4 | $-\sqrt{1/3}$ | $-\sqrt{1/3}$ | 1 |
| | $\sqrt{1/3}$ | $-\sqrt{1/3}$ | 1 |
| | $-\sqrt{1/3}$ | $\sqrt{1/3}$ | 1 |
| | $\sqrt{1/3}$ | $\sqrt{1/3}$ | 1 |
| 3 | 0.5 | 0 | 1/6 |
| | 0 | 0.5 | 1/6 |
| | 0.5 | 0.5 | 1/6 |

10

- Using chain rule, the $\xi$ and $\eta$ derivatives of the i$^{th}$ shape function in terms of x and y derivatives is as follows

$$
\begin{Bmatrix} \dfrac{\partial S_i}{\partial x} \\ \dfrac{\partial S_i}{\partial x} \end{Bmatrix} = \begin{Bmatrix} \dfrac{\partial \xi}{\partial x} & \dfrac{\partial \eta}{\partial x} \\ \dfrac{\partial \xi}{\partial y} & \dfrac{\partial \eta}{\partial y} \end{Bmatrix} \begin{Bmatrix} \dfrac{\partial S_i}{\partial \xi} \\ \dfrac{\partial S_i}{\partial \eta} \end{Bmatrix} = [J^e]^{-1} \begin{Bmatrix} \dfrac{\partial S_i}{\partial \xi} \\ \dfrac{\partial S_i}{\partial \eta} \end{Bmatrix}
$$

Where $[J^e]$ is the Jacobian matrix

Hence after substituting the above equations in the stiffness element equation, the following form is obtained

$K_{ij}^e$

$$
= \int_{\Omega^e} \left\{ S_i \left[ u_x \left( [J^e]^{-1}{}_{11} \frac{\partial S_j}{\partial \xi} + [J^e]^{-1}{}_{12} \frac{\partial S_j}{\partial \eta} \right) + u_y \left( [J^e]^{-1}{}_{21} \frac{\partial S_j}{\partial \xi} + [J^e]^{-1}{}_{22} \frac{\partial S_j}{\partial \eta} \right) \right] \right.
$$

$$
+ D \left[ \left( [J^e]^{-1}{}_{11} \frac{\partial S_i}{\partial \xi} + [J^e]^{-1}{}_{12} \frac{\partial S_i}{\partial \eta} \right) \left( [J^e]^{-1}{}_{11} \frac{\partial S_j}{\partial \xi} + [J^e]^{-1}{}_{12} \frac{\partial S_j}{\partial \eta} \right) \right.
$$

$$
\left. \left. + \left( [J^e]^{-1}{}_{21} \frac{\partial S_i}{\partial \xi} + [J^e]^{-1}{}_{22} \frac{\partial S_i}{\partial \eta} \right) \left( [J^e]^{-1}{}_{21} \frac{\partial S_j}{\partial \xi} + [J^e]^{-1}{}_{22} \frac{\partial S_j}{\partial \eta} \right) \right] \right\} |J^e| d\xi d\eta
$$

- So each element of the local stiffness matrix is computed and then they are assembled to the global stiffness matrix according to the global node numbers of any element
- Appropriate initial and boundary conditions are applied and the matrix equation is solved to obtain the values for the unknown vector.

# Chapter 4

# Numerical Model

## 4.1 Model description

A micro model representing the pore scale subsurface environment was developed. It has a size of 1cm × 8.8mm with two inlets and an outlet. It has 100 μm equally spaced 300 μm diameter pores. The CAD file of the model was used for the simulations. Neumann and Dirchlet boundary conditions were used at the inlets and outlets while the rest of boundaries have no flux condition for simulating fluid flow. The model was initially filled with a fixed concentration of chromium and substrate while the bacteria was given as a flux at point inside the model.

## 4.2 Equations used

### 4.2.1 Fluid flow

Fluid flow was modeled using the Navier-Stokes equations on bulk liquid that is considered to be an incompressible Newtonian fluid. The property of each is mentioned below

$$\frac{\partial u}{\partial t} + u.\nabla u = -\frac{\nabla p}{\rho} + \nu\nabla^2 u$$

transient   inertia   pressure   diffusion

Continuity equation for conservation of momentum

$$\nabla.u = 0$$

Reynold's number $R_e$ given by

$$R_e = \frac{\rho v d}{\mu} = \frac{10^3 \times 0.0002 \times 100 \times 10^{-6}}{8.6 \times 10^{-4}} = 0.023$$

for a maximum velocity of 0.2mm/s

As $R_e$ <1, inertial forces are negligible and the inertia term in NS equation is neglected

### 4.2.1 Substrate and Chromium transport

The transport and biotransformation of substrate and Cr VI is modeled using the advection-diffusion-reaction equation. The reaction term represents the consumption

of substrate by bacteria in the substrate transport equation and biotransformation of Cr VI to Cr III in Chromium transport equation. [23-24]

- For substrate

$$\frac{\partial C_s}{\partial t} = D_s \nabla^2 C_s - \nabla(\boldsymbol{u} C_s) - k_s$$

$$\text{where } k_s = \frac{\mu_{max} M}{Y} \frac{C_s}{C_s + K_s} \frac{K_i}{C_{cr} + K_i}$$

- For Chromium

$$\frac{\partial C_{Cr}}{\partial t} = D_{Cr} \nabla^2 C_{Cr} - \nabla(\boldsymbol{u} C_{Cr}) - \eta k_s$$

### 4.2.2 Biomass spread and growth

Biomass spread and growth is modeled using the advection-diffusion-reaction term and the reaction represents the growth and decay of bacteria.

$$\frac{\partial M}{\partial t} = D_s \nabla^2 M - \nabla(\boldsymbol{u} M) + \mu_{max} M \frac{C_s}{C_s + K_s} \frac{K_i}{C_{cr} + K_i} - K_D M$$

## 4.3 Model inputs

Constants used are as follows

**Table 4.1 Model inputs used**

| Paramater | Description | Value |
|---|---|---|
| $K_s$ | Half-maximum-rate concentration of substrate (mg/L of COD) | 40 |
| $Y$ | Biomass yield coefficient | 0.263 |
| $\mu_{max}$ | Maximum specific growth rate of biomass (h$^{-1}$) | 0.3 |
| $k_d$ | Inactivation coefficient (h$^{-1}$) | 0.0025 |
| $D_S$ | Diffusion coefficient of species i within the water (m$^2$/d) | $3.6 \times 10^{-8}$ |
| $D_{Cr}$ | | $3.2 \times 10^{-10}$ |
| $D_m$ | | $6 \times 10^{-11}$ |
| $S_S$ | Concentration of chemical species i in the influent (mg/L) | 2000 |
| $S_{Cr}$ | | 100-500 |
| $S_M$ | | 15 |
| $v_{in}$ | Average velocity at the inlets (m/h) | 0.72 |
| $\rho$ | Water density (kg/m$^3$) | 1000 |
| $\mu$ | Dynamic viscosity of water (N-h/m$^2$) | $2.4 \times 10^{-7}$ |
| $\nu$ | Kinematic viscosity of water (m$^2$/h) | 0.00375 |

[20-21]

## 4.4    COMSOL Model

COMSOL was used to develop the numerical model. The software is an FEM based solver that allows physics-based user interfaces and coupled systems of partial differential equations.

The solving process is as follows
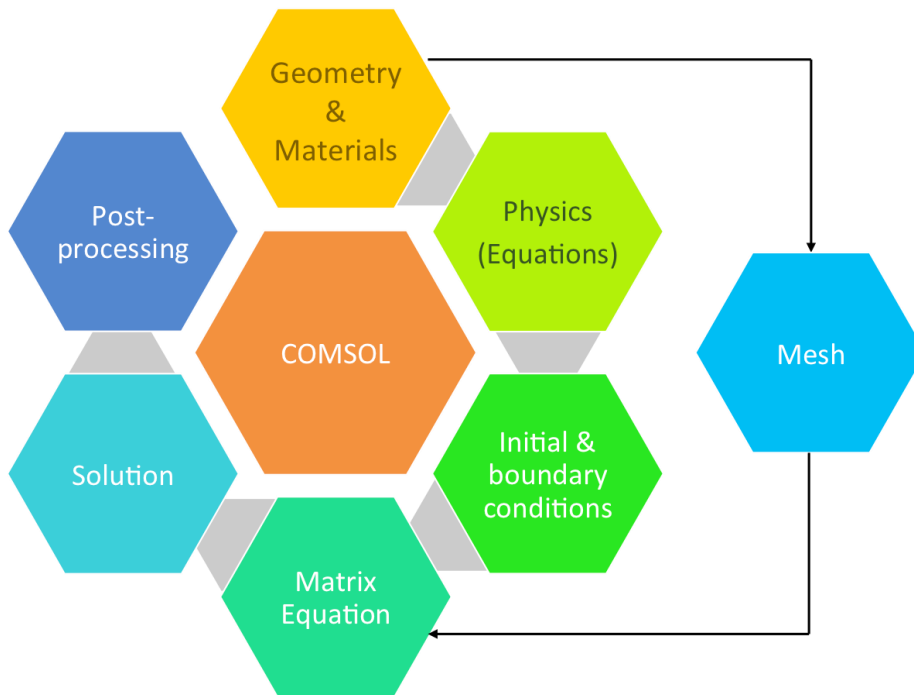


**Figure 4.1 COMSOL working process**

The unstructured mesh developed for the model has 1757 quadrilateral elements and 5022 triangular elements amounting to a total of 6779 elements (1802 edge and 818 vertex elements). Minimum element quality being 0.04352 and average element quality is 0.6136. Maximum and minimum element sizes are 2130 μm and 171 μm respectively.

# Chapter 5

# Results and discussions

## 5.1 Model 1

A homogeneous model with inlet velocity of $1\times10^{-9}$m/s, initial substrate concentration of 2000mg/L, initial biomass concentration of 20mg/L and initial Cr (VI) concentration of 100mg/L. The inoculation point was at the center of the biomass area. Simulation time period was 1 day for an interval of 0.2 hours.
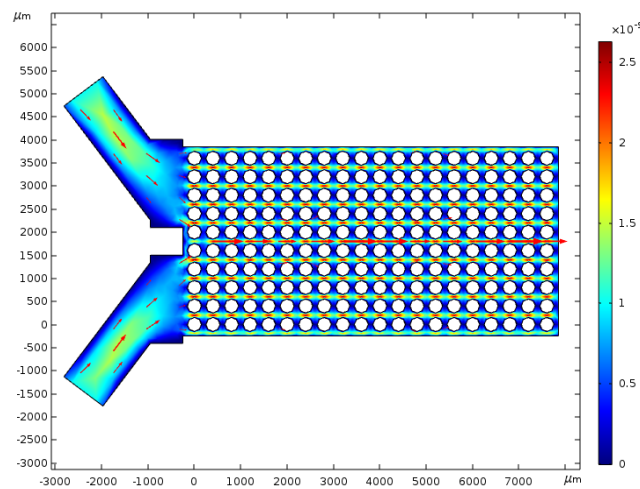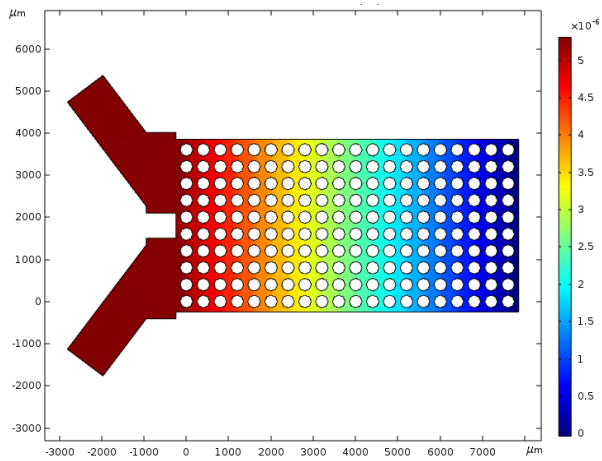


**Figure 5.1 Velocity magnitude (m/s)**

**Figure 5.2 Pressure plot (Pa)**

Figure 5.1 shows the increase in velocity between the pores due to decrease in channel width for the movement of water. Figure 5.2 shows the pressure variation across the model. The pressure varies from 5.5 μPa at the inlet to almost 0 Pa at the outlet. Due to low fluid velocity the pressure is quite low. Figure 5.3 is the biomass plot which show the spread of the bacteria after 24 hours.
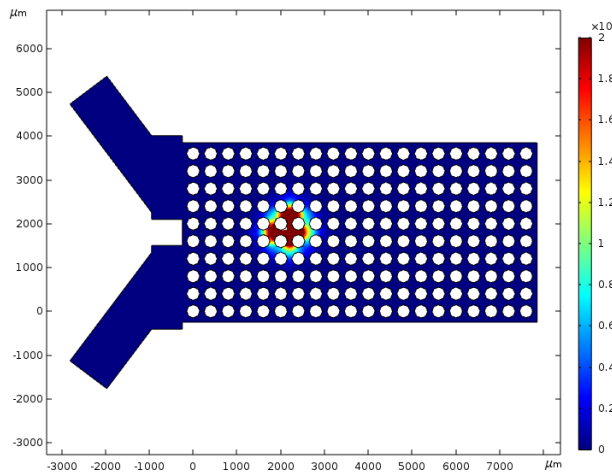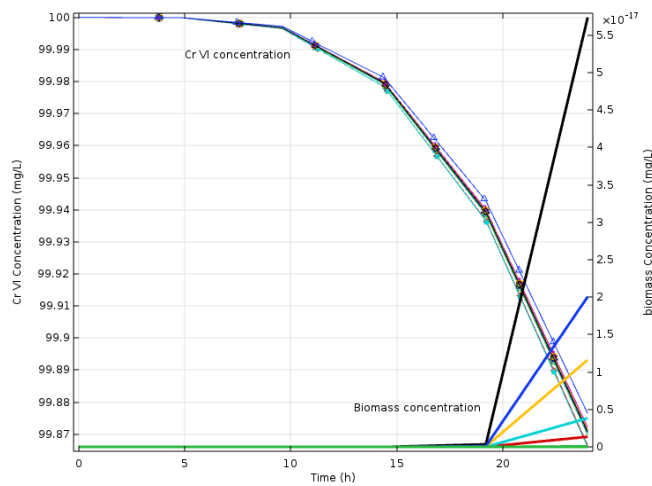


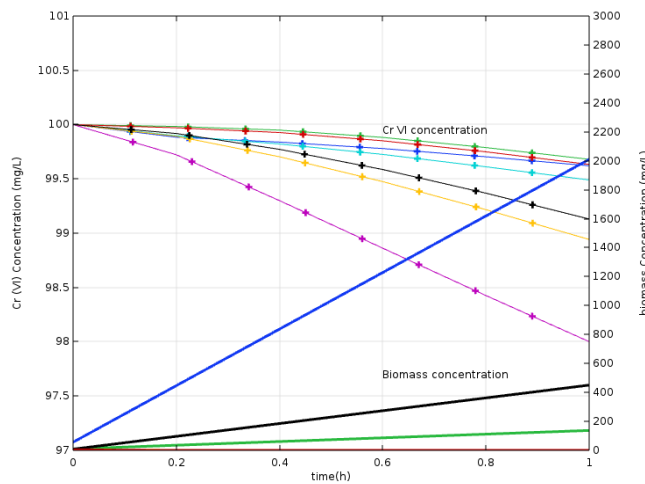**Figure 5.3 Biomass concentration plot (mg/L)**
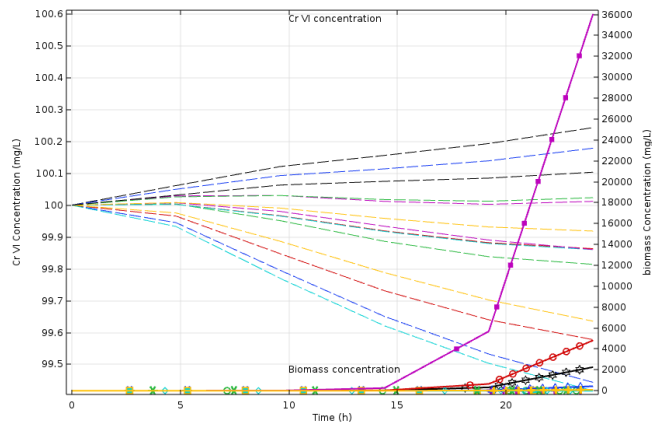
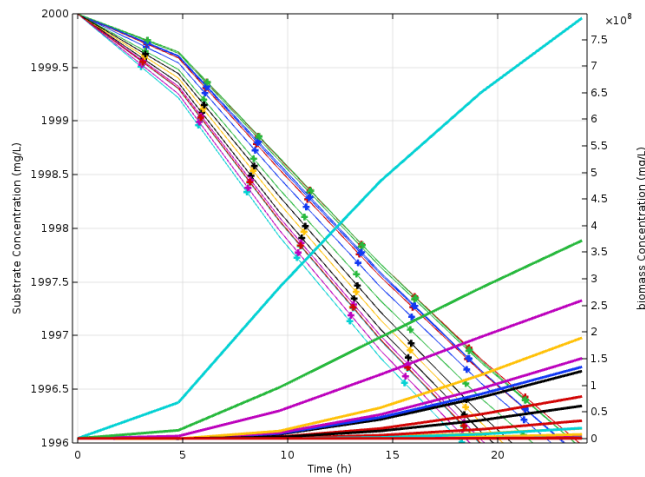**Figure 5.4 Cr VI Concentration (mg/L) Cr (VI) & Biomass concentration(mg/L) wrt time near inlet (1 day)**

Figure 5.4 is a plot of Cr (VI) and biomass concentration with respect to time at a few locations near the inlet. There is no significant change in biomass concentration until 12 hours as the bacteria inoculation point is located beyond the inlet and the time lag is due to the time taken for the bacteria to diffuse near the inlet locations and then grow. There decrease in Cr (VI) concentration due to advection in the beginning and biotransformation in the later stages.



**Figure 5.5 Cr VI Concentration (mg/L) Cr VI & Biomass concentration(mg/L) wrt time near outlet (1 day)**

**Figure 5.6 Cr(VI) Concentration (mg/L) Cr VI & Biomass concentration(mg/L) wrt time at near the inoculation point (1 day)**
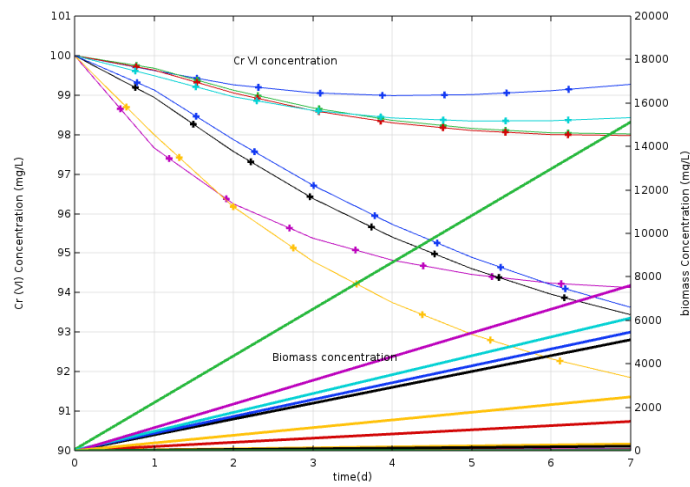


**Figure 5.7 Substrate (mg/L) & Biomass (mg/L) concentration wrt time at near the inoculation point**

Figure 5.5 is a plot of Cr (VI) and biomass concentration with respect to time at a few locations near the outlet. The biomass growth doesn't occur until after 18 hours. This is due to the lag in movement of the biomass from the inoculation point to the outlet owing to the very low velocity. There is a gradual decrease in the Cr (VI) concentration at the beginning due to its exit from the model through the outlet and the steep decrease later due to biotransformation by bacteria. Figure 5.6 is a plot of Cr (VI) and biomass concentration with respect to time at a few locations near the inoculation point. The gradual decrease in Cr (VI) due to biotransformation by the increasing biomass can be observed. Figure 5.7 is a plot of substrate and biomass concentration with respect to time at a few locations near the inoculation point. A gradual decrease in substrate concentration is seen with immediate increase in biomass concentration as it is near to the inoculation point.

18

## 5.2 Model 1

A homogeneous model with inlet velocity of $1 \times 10^{-9}$m/s, initial substrate concentration of 2000mg/L, initial biomass concentration of 20mg/L and initial Cr (VI) concentration of 100mg/L. The inoculation point was at the center of the biomass area. Simulation time period was 7 days with an interval of 1 day.

Figure 5.8 and figure 5.9 are plots of Cr (VI) and biomass concentration with respect to time at a few locations near the inoculation point and the inlet. The plots show gradual decrease of Cr (VI) concentration is seen along with steady increase in biomass concentration.



**Figure 5.8Cr(VI) Concentration (mg/L) Cr VI & Biomass concentration(mg/L) wrt time at near the inoculation point (7 days)**
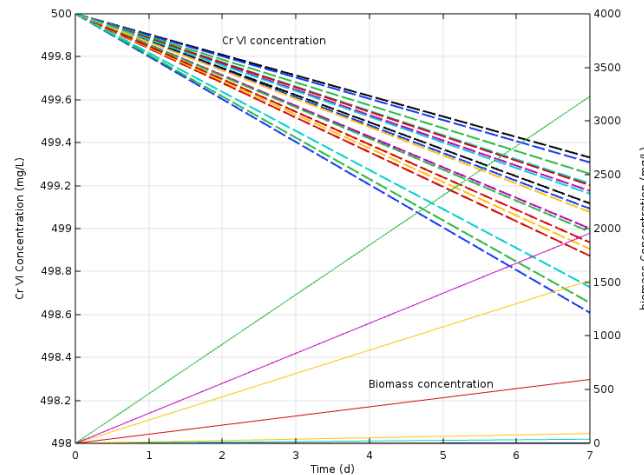


**Figure 5.9 Cr VI Concentration (mg/L) Cr (VI) & Biomass concentration(mg/L) wrt time near inlet (7 days)**
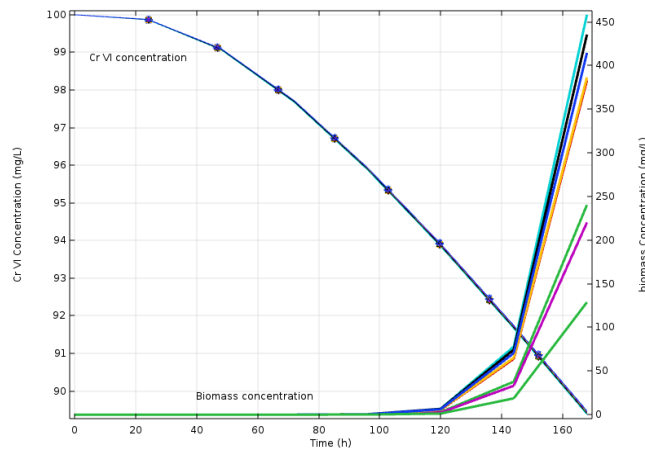
**Figure 5.10 Cr VI Concentration (mg/L) Cr (VI) & Biomass concentration(mg/L) wrt time near outlet (7 days)**

Figure 5.10 is a plot of Cr (VI) and biomass concentration with respect to time at a few locations near the outlet, in which gradual decrease of Cr (VI) concentration initially as it gets flushed out at the outlet and steeper decrease later due to biotransformation by bacteria. There is no change in the concentration of biomass until 100 hours as the bacteria movement from the inoculation point to the outlet is very slow due to considerably low velocities inside the model. There is steep rise in biomass growth later which accounts for the sharper decrease in Cr (VI) concentration.

## 5.3 Model 1

A homogeneous model with inlet velocity of $1 \times 10^{-9}$m/s, initial substrate concentration of 2000mg/L, initial biomass concentration of 20mg/L and initial Cr (VI) concentration of 500mg/L. The inoculation point was at the center of the biomass area. Simulation time period was 28 days with an interval of 1 day
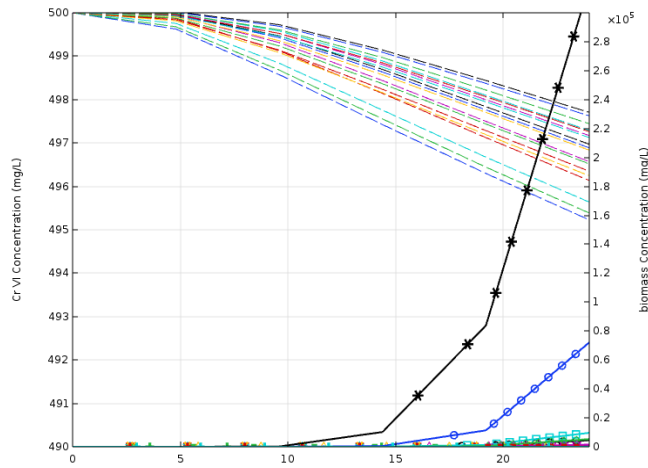
Figure 5.11 and figure 5.12 are plots of Cr (VI) and biomass concentration with respect to time at a few locations near the inoculation point and the inlet. General trend of the plots depict decrease in Cr (VI) concentration with increasing biomass concentration.

**Figure 5.11 Cr VI Concentration (mg/L) Cr (VI) & Biomass concentration(mg/L) wrt time near inlet (28 days)**
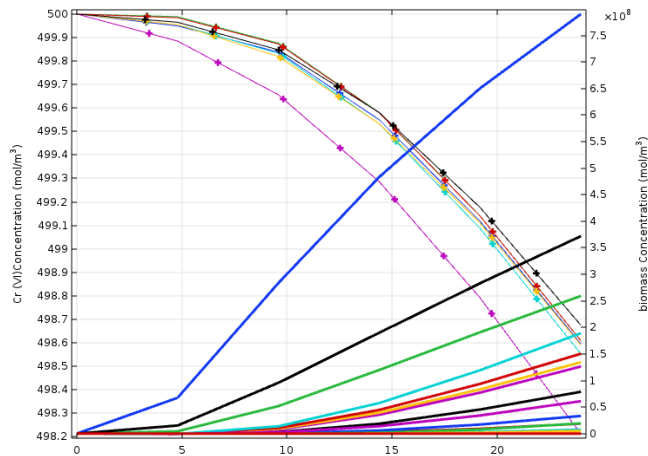


**Figure 5.12 Cr (VI)Concentration (mg/L) Cr VI & Biomass concentration wrt time at near the inoculation point (28 days)**
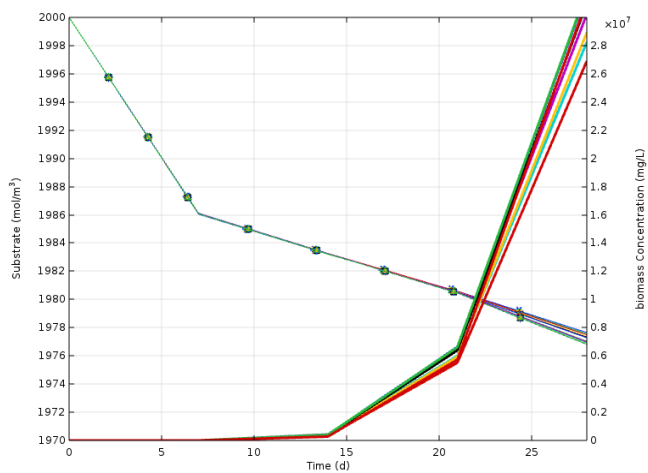


**Figure 5.13 Substrate (mg/L) Cr VI & Biomass concentration(mg/L) wrt time near outlet (28 days)**

21

Figure 5.13 is a plot of substrate and biomass concentration with respect to time at a few locations near the outlet. A gradual decrease in substrate concentration is seen with increase in biomass concentration after a lag as it is near to the outlet.

# Chapter 6

# Conclusions and future work

- The model developed can predict the velocity and pressure profiles developed fairly well.
- It can also predict the movement and, consumption of the substrate and biotransformation of Cr (VI) by bacteria along with the changes in its concentration. The model can be applied on other pore scale setups as well.

- The model can be improved by modelling bacteria movement using cellular automata, thus accounting for its mobility (tumbling of bacteria).
- Chemotaxis of bacteria towards the contaminant and substrate can also be modelled to improve the biomass spread direction
- Clogging due to biomass as well as it attachment and detachment to the pores changes the fluid flow dynamics, incorporation of this aspect into the model can improve in substantially.
- The model can be validated with experimental results and inverse modelling can be done to estimate parameters known to check the accuracy and applicability of the model.

# References

[1] Philip, L. (2010). DEVELOPMENT OF MATHEMATICAL MODELS FOR CLEAN UP OF Cr (VI) CONTAMINATED AQUIFERS USING BIOREMEDIATION Final Report Submitted to Indian National Committee on Ground Water Ministry of Water Resources GOVERNMENT OF INDIA By and Environmental and Water Reso, (Vi).

[2] Chen, J. M., & Hao, O. J. (1998). Microbial chromium (VI) reduction. *Critical Reviews in Environmental Science and Technology*, *28*(3), 219-251.

[3] Fruchter, J. (2002). Peer reviewed: In-situ treatment of chromium-contaminated groundwater.

[4] Knutson, C. E., Werth, C. J., & Valocchi, A. J. (2005). Pore-scale simulation of biomass growth along the transverse mixing zone of a model two-dimensional porous medium. *Water Resources Research*, *41*(7), 1–12.

[5] Tang, Y., Valocchi, A. J., Werth, C. J., & Liu, H. (2013). An improved pore-scale biofilm model and comparison with a microfluidic flow cell experiment. *Water Resources Research*, *49*(12), 8370–8382.

[6] Qin, C. Z., & Hassanizadeh, S. M. (2015). Pore-Network Modeling of Solute Transport and Biofilm Growth in Porous Media. *Transport in Porous Media*, *110*(3), 345–367.

[7] Geiger, S., Roberts, S., Matthäi, S. K., Zoppou, C., & Burri, A. (2004). Combining finite element and finite volume methods for efficient multiphase flow simulations in highly heterogeneous and structurally complex geologic media. *Geofluids*, *4*(4), 284-299.

[8] Ling, B., Bao, J., Oostrom, M., Battiato, I., & Tartakovsky, A. M. (2017). Modeling variability in porescale multiphase flow experiments. *Advances in Water Resources*, *105*, 29–38.

[9] Tang, Y., Zhao, H., Marcus, A. K., Krajmalnik-Brown, R., & Rittmann, B. E. (2012). A steady-state biofilm model for simultaneous reduction of nitrate and perchlorate, part 1: Model development and numerical solution. *Environmental Science and Technology*, *46*(3), 1598–1607.

[10]        Tang, Y., Zhao, H., Marcus, A. K., Krajmalnik-Brown, R., & Rittmann, B. E. (2012). A steady-state biofilm model for simultaneous reduction of nitrate and perchlorate, part 2: Parameter optimization and results and discussion. *Environmental Science and Technology*, *46*(3), 1608–1615.

[11]        Beyenal, H., & Lewandowski, Z. (2005). Modeling mass transport and microbial activity in stratified biofilms. *Chemical Engineering Science*, *60*(15), 4337–4348.

[12]        Kang, Q., Lichtner, P. C., & Zhang, D. (2007). An improved lattice Boltzmann model for multicomponent reactive transport in porous media at the pore scale. *Water Resources Research*, *43*(12), 1–12.

[13]        Kang, Q., Lichtner, P. C., & Zhang, D. (2006). Lattice Boltzmann pore-scale model for multicomponent reactive transport in porous media. *Journal of Geophysical Research: Solid Earth*, *111*(B5).

[14]        Zhang, X., Wang, X., & Sun, Q. (2017). Modeling of biofilm growth on ager substrate using the extended finite element method. *Procedia IUTAM*, *23*, 33-41.

[15]        Chen-Charpentier, B. (1999). Numerical simulation of biofilm growth in porous media. *Journal of computational and applied mathematics*, *103*(1), 55-66.

[16]        Ezeuko, C. C., Sen, A., Grigoryan, A., & Gates, I. D. (2011). Pore-network modeling of biofilm evolution in porous media. *Biotechnology and bioengineering*, *108*(10), 2413-2423.

[17]        Carrel, M., Morales, V. L., Dentz, M., Derlon, N., Morgenroth, E., & Holzner, M. (2018). Pore-Scale Hydrodynamics in a Progressively Bioclogged Three-Dimensional Porous Medium: 3-D Particle Tracking Experiments and Stochastic Transport Modeling. *Water resources research*, *54*(3), 2183-2198.

[18]        Gharasoo, M. G. (n.d.). *development and application of a pore-network model Mehdi Gholami Gharasoo Reactive transport simulations of microbial activity and biogeochemical transformations in porous environments*

[19]        Zhang, C., Kang, Q., Wang, X., Zilles, J. L., Müller, R. H., & Werth, C. J. (2010). Effects of pore-scale heterogeneity and transverse mixing on bacterial growth in porous media. *Environmental Science and Technology*, *44*(8), 3085–3092.

[20]        Shashidhar, T., Philip, L., & Bhallamudi, S. M. (2006). Bench-scale column experiments to study the containment of Cr (VI) in confined aquifers by bio-transformation. *Journal of hazardous materials*, *131*(1-3), 200-209.

[21] Shashidhar, T., Bhallamudi, S. M., & Philip, L. (2007). Development and validation of a model of bio-barriers for remediation of Cr (VI) contaminated aquifers using laboratory column experiments. *Journal of hazardous materials*, *145*(3), 437-452.

[22] http://users.metu.edu.tr/csert/me582/ME582%20Ch%2002.pdf